New Directions in Linear Acoustics and Vibration

Quantum Chaos, Random Matrix Theory, and Complexity

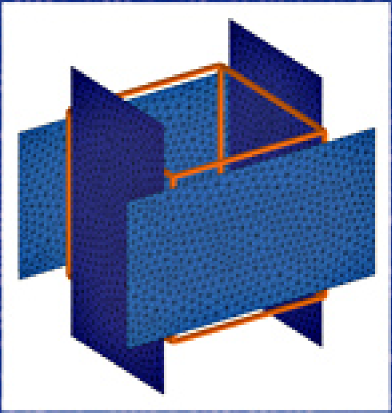

Edited by
Matthew Wright & Richard Weaver

CAMBRIDGE

CAMBRIDGE www.cambridge.org/9780521885089

This page intentionally left blank

NEW DIRECTIONS IN LINEAR ACOUSTICS AND VIBRATION

The field of acoustics is of immense industrial and scientific importance. The subject is built on the foundations of linear acoustics, which is widely regarded as so mature that it is fully encapsulated in the physics texts of the 1950s. This view was changed by developments in physics such as the study of quantum chaos. Developments in physics throughout the last four decades, often equally applicable to both quantum and linear acoustic problems but overwhelmingly more often expressed in the language of the former, have explored this. There is a significant new amount of theory that can be used to address problems in linear acoustics and vibration, but only a small amount of reported work does so. This book is an attempt to bridge the gap between theoreticians and practitioners, as well as the gap between quantum and acoustic. Tutorial chapters provide introductions to each of the major aspects of the physical theory and are written using the appropriate terminology of the acoustical community. The book will act as a quick-start guide to the new methods while providing a wide-ranging introduction to the physical concepts.

Matthew Wright is a senior lecturer in Acoustics at the Institute of Sound and Vibration Research (ISVR). His B.Eng. was in engineering acoustics and vibration, and his Ph.D. was in Volterra series characterization and identification of nonlinear bioacoustic systems, both from the University of Southampton. Since then he has worked on flow control for drag and noise reduction, turbofan inlet design, aeroacoustic theory, violin acoustics, and quantum chaos in acoustics, for the study of which he was awarded an EPSRC Advanced Research Fellowship. His current interests include wind farm noise and the neuroscience of hearing. He is a Fellow of the Institute of Acoustics, a Fellow of the Institute of Mathematics and Its Applications, a Senior Member of the American Institute of Aeronautics and Astronautics, a Member of the Acoustical Society of America, and the book reviews editor of the *Journal of Sound and Vibration*. He teaches musical instrument acoustics and acoustical design.

Richard Weaver received an A.B. degree in physics from Washington University in St. Louis in 1971 and a Ph.D. in astrophysics from Cornell University in 1977. He has been at the University of Illinois since 1981, after a research associateship in theoretical elastic wave propagation and ultrasonics at Cornell. He was elected a Fellow of the Acoustical Society of America in 1996 and received the Hetényi Award from the Society for Experimental Mechanics in 2004. He is associate editor of the *Journal of the Acoustical Society of America.*

New Directions in Linear Acoustics and Vibration

QUANTUM CHAOS, RANDOM MATRIX THEORY, AND COMPLEXITY

Edited by

Matthew Wright

University of Southampton

Richard Weaver

University of Illinois

CAMBRIDGE
UNIVERSITY PRESS

CAMBRIDGE UNIVERSITY PRESS
Cambridge, New York, Melbourne, Madrid, Cape Town, Singapore,
São Paulo, Delhi, Dubai, Tokyo

Cambridge University Press
The Edinburgh Building, Cambridge CB2 8RU, UK

Published in the United States of America by Cambridge University Press, New York

www.cambridge.org
Information on this title: www.cambridge.org/9780521885089

First published in print format 2010

ISBN-13 978-0-511-78477-4 eBook (Adobe Reader)

ISBN-13 978-0-521-88508-9 Hardback

Contents

Foreword by Michael Berry — *page* vii

Introduction 1
Matthew Wright and Richard Weaver

1 **The Semiclassical Trace Formula** 5
Matthew Wright

2 **Wave Chaos for the Helmholtz Equation** 24
Olivier Legrand and Fabrice Mortessagne

3 **The Unreasonable Effectiveness of Random Matrix Theory for the Vibrations and Acoustics of Complex Structures** 42
Richard Weaver

4 **Gaussian Random Wavefields and the Ergodic Mode Hypothesis** 59
Mark R. Dennis

5 **Short Periodic Orbit Theory of Eigenfunctions** 77
Eduardo G. Vergini and Gabriel G. Carlo

6 **Chaotic Wave Scattering** 96
Jonathan P. Keating and Marcel Novaes

7 **Transfer Operators Applied to Elastic Plate Vibrations** 110
Niels Søndergaard

8 **Mesoscopics in Acoustics** 123
Richard Weaver

9 **Diagrammatic Methods in Multiple Scattering** 131
Joseph A. Turner and Goutam Ghoshal

10 **Time-Reversed Waves in Complex Media** 146
Mathias Fink

11 **Ocean Acoustics: A Novel Laboratory for Wave Chaos** 169
Steven Tomsovic and Michael Brown

12 **Mesoscopic Seismic Waves** 188
Michel Campillo and Ludovic Margerin

13 **Random Matrices in Structural Acoustics** 206
Christian Soize

14 **The Analysis of Random Built-Up Engineering Systems** 231
Robin Langley

References 251

Index 271

Foreword

Michael Berry

H. H. Wills Physics Laboratory, University of Bristol, Bristol, UK

In the early 1970s, Martin Gutzwiller and Roger Balian and Claude Bloch described quantum spectra in terms of classical periodic orbits, and in the mid 1970s it became clear that the random matrix theory devised for nuclear physics would also describe the statistics of quantum energy levels in classically chaotic systems. It seemed obvious even then that these two great ideas would find application in acoustics, but it has taken more than three decades for this insight to be fully implemented. The chapters in this fine collection provide abundant demonstration of the continuing fertility, in the understanding of acoustic spectra, of periodic orbit theory and the statistical approach. The editors' kind invitation to me to write this foreword provides an opportunity to make a remark about each of these two themes.

First, here is a simple argument for periodic orbit theory being the uniquely appropriate tool for describing the acoustics of rooms. The reason for confining music and speech within auditoriums – at least in climates where there is no need to protect listeners from the weather – is to prevent sound from being attentuated by radiating into the open air. But if the confinement were perfect, that is, if the walls of the room were completely reflecting, sounds would reverberate forever and get confused. To avoid these extremes, the walls in a real room must be partially absorbing. This has the effect of converting the discrete eigenvalues with perfectly reflecting walls into resonances. I will argue that for real rooms the width of resonances usually exceeds their spacing. This is important because it casts doubt on the usefulness of the concept of an individual mode in assessing the acoustic response of rooms; a smoothed description of the spectrum seems preferable. But smoothing is precisely what periodic orbit theory naturally describes. When there is no absorption, the contributions from the long periodic orbits make the convergence of the sum problematic, frustrating the direct calculation of individual eigenvalues, for example, in quantum chaology. Absorption attentuates the long orbits, and the oscillatory contributions from few shortest orbits are sufficient to describe the acoustic response. But these few orbits are important: the crudest smoothing, based simply on the average spectral density, obliterates all the spectral oscillations and fails to capture the characteristics of most real rooms.

To assess the significance of absorption, start from the Weyl counting formula for the number N of modes with frequencies less than f, for a room of volume L^3:

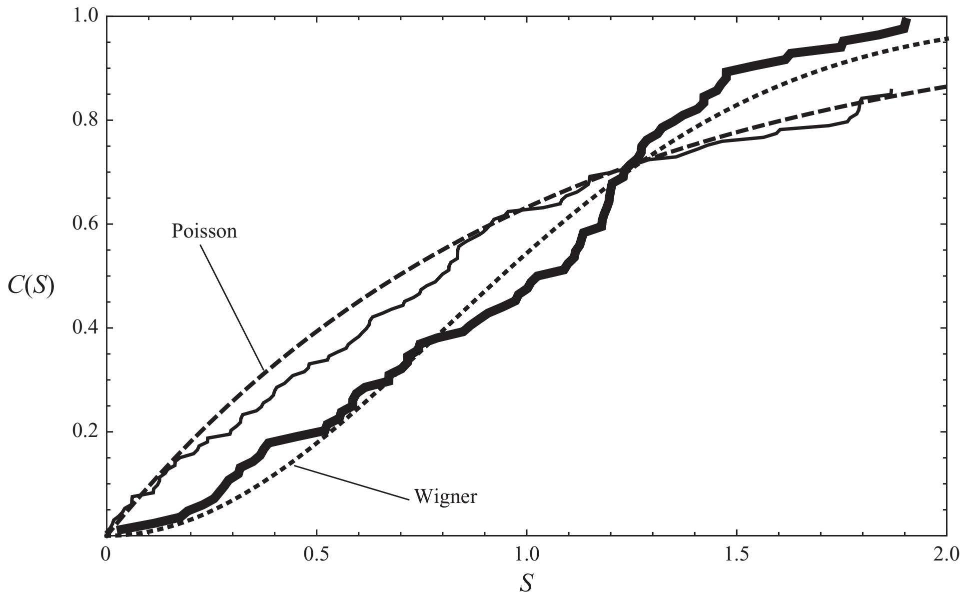

if the speed of sound is $c = 330\,\mathrm{ms}^{-1}$,

$$N = \frac{4\pi L^3 f^3}{3c^3}.$$

In the presence of absorption, modeled approximately by an exponential amplitude decay time T, that is, intensity $\sim \exp(-2t/T)$, the resonance width corresponds to a frequency broadening,

$$\Delta f = \frac{1}{2\pi T}.$$

Thus, incorporating the reverberation time T_{60}, corresponding to 60-dB intensity reduction, that is, $T = T_{60}/3\log_e 10$, the number ΔN of modes smoothed over by the broadening is

$$\Delta N = 6\log_e 10\frac{L^3 f^2}{c^3 T_{60}}.$$

For estimates, we can choose the frequency middle A ($f = 440\,\mathrm{Hz}$). Then, for a small auditorium with $L = 6\,\mathrm{m}$, and a reverberation time $T_{60} = 0.7\,\mathrm{s}$, $\Delta N \sim 23$, which is unexpectedly large for such a small room. For the Albert Hall in London, where the effective $L \sim 60\,\mathrm{m}$, and taking $T_{60} = 2\,\mathrm{s}$, $\Delta N \sim 8{,}200$. These estimates strongly suggest that there is little sense in studying individual modes.

Second, here is an unusual application of spectral statistics from 1993, inspired by a visit to Loughborough University, where I talked about quantum chaos and mentioned that the ideas could be usefully applied in acoustics. Afterward, Robert Perrin showed me his measurements (Perrin et al. 1983) of eigenfrequencies of one English church bell, ranging from 292.72 Hz – the lowest mode, called the hum, through the first few harmonics, with their traditional names Fundamental, Tierce, Quint, Nominal, Twister, Superquint – up to the 134th frequency of 9,285 Hz. This provided sufficient data to make a first attempt to understand the frequency spacings distribution.

I did this in two ways. First, taking the whole set of 134 frequencies, unfolding them by fitting the counting function (spectral staircase) to a cubic function, and then calculating the 133 spacings, normalized to unit mean. The resulting cumulative spacings distribution $C(S) =$ fraction of spacings less than S, fits the Poisson distribution $1 - \exp(-S)$ reasonably well (the thin and dashed curves in the figure). This is not surprising because the bell has approximate rotation symmetry, and the whole set of frequencies conflates subsets with different numbers l of nodal meridians ("angular momentum quantum number"). Fortunately the value of l for each frequency was given; l ranged from 0 to 28, but only the subsets with $0 \leq l \leq 10$ included sufficient frequencies to generate sensible statistics. In the second procedure, I unfolded these subsets separately and conflated the spacings afterwards, thereby generating the heavy curve in the figure. This is better fitted to the Wigner cumulative distribution $1 - \exp(-S^2/4)$ (the dotted curve in the figure), indicating strong repulsion of neighboring frequencies in each l-subset. The precise fit is not important because the Wigner distribution should apply when the ray geodesics on the bell – "classical paths" – are chaotic, whereas the vibrations of the bell, regarded as a thin elastic sheet, are probably integrable, with frequencies given by the modes of a one-dimensional "radial" equation, albeit of fourth order.

Reference

Perrin, R., Charnley, T. & DePont, L. (1983), "Normal modes of the modern English church bell," *J. Sound. Vib.* **90**, 29–49.

Introduction

Matthew Wright and Richard Weaver

This book has some of its genesis in the, possibly apocryphal, story that at an acoustics conference in the late 1980s a certain distinguished professor, tiring of the proceedings, turned to the assembled researchers and announced

> Listen! If what you're doing isn't nonlinear or transonic, then don't bother! It's all been done!

Certainly it has become easy to think of linear acoustics as essentially completed. After all, classic texts such as Morse and Feshbach (1953) give admirably thorough expositions of very general techniques, particularly those based on Green's functions. Cases described by coordinate systems in which the governing equations are separable are extensively tabulated and admit analytic solutions. The alternative is to employ numerical methods, many of them also based on Green's functions, which work in arbitrarily complex geometries. There is perhaps a perception that notwithstanding a host of important applied problems, there are no fundamental issues remaining in linear acoustics. Increased understanding of the richness and complexity of nonlinear problems with the explosion of interest in chaos only serves to make linear systems seem "done and dusted" in comparison.

And yet this picture is overly dismissive. A solution of a linear differential equation depends nonlinearly on its coefficients and the shape of the boundary. The dependence is all the richer if those coefficients are random or if boundary reflections are defocusing. Developments in physics throughout the last four decades, often equally applicable to both quantum and linear acoustic problems, but overwhelmingly more often expressed in the language of the former, have explored this. More than that they have provided a new way of thinking about such things. We have been impressed at the significant new body of theory that can be used to address problems in linear acoustics and vibration, although also disappointed at the small amount of reported work that does so. This book is an attempt to bridge the gap between theoreticians and practitioners, as well as the gap between quantum and acoustic, a gap that is mostly terminological but should nevertheless not be underestimated. Our hope is that acousticians and vibration engineers who wish to see what can be done with these new tools will find in this book a comprehensible introduction and that physicists may also learn what problems might usefully be addressed.

So what is on offer? We would like to take the reader on a short guided tour of the terrain. We begin with what is known as the *semiclassical trace formula* (Chapter 1), which expresses the modal density of a closed, lossless enclosure (membrane or cavity) in terms of its *periodic orbits*, closed internal ray paths that repeat indefinitely. As a way to determine eigenvalues (let alone response to arbitrary excitations) it cannot compete with the numerical techniques that have been refined for use in engineering (such as finite elements) or physics (such as plane-wave decomposition); its significance lies in the fact that it provides an explicit link between the shape of an enclosure and its acoustic characteristics, both in an average sense (via the Weyl series) and at the level of individual eigenvalues, and in a way that doesn't depend on separability.

This connection is important because for many shapes the periodic orbits are unstable and the ray paths are *chaotic*, the implications of which are explored in Chapter 2. It can be disconcerting to find chaos having such a profound influence on linear systems. This is due to the nonlinearity of ray motion in the high-frequency limit, and the study of the effects of this on the finite-frequency wave motion has come to be known as quantum chaology or (despite linguistic objections) *quantum chaos*. It used to be easy to imagine that almost all ordinary differential equations had well-behaved, predictable solutions because almost all the ones in books did. That misapprehension was shattered by the explosion of awareness about chaos. In the same way it is easy to fall into the trap of thinking that modeshapes and natural frequencies are as simple and regular in arbitrary shapes as those of the simple textbook examples used to teach the subject. They are not, and for very similar reasons.

One of the consequences of chaotic ray motion is that eigenfunctions often resemble superpositions of Gaussian random waves, the properties of which are explored in more detail in Chapter 4. Those that do not are referred to as "scarred modes"; Chapter 5 presents an ingenious formulation that allows the eigenfunctions to be represented with impressive efficiency in a basis built out of deliberately constructed scar functions. Of course acousticians rarely encounter truly lossless systems in practice; so some of the implications of opening the enclosure are explored in Chapter 6. And in Chapter 7 the central result of the periodic orbit theory is re-derived in a form suitable for elasticity so as to expand the range of possible applications.

Before that, however, we introduce the second major theme of this book: *random matrix theory*. The study of the statistics of the eigenvalues of ensembles of matrices whose elements are random variables and exhibit a particular symmetry began in nuclear physics as an exploration of the conjecture that a sufficiently complex system might have properties statistically similar to those of a random Hamiltonian. Modern computational capabilities have made it easier to test conjectures and confirm analytic results. For example, the fact that the normalized spacings of the eigenvalues of a large Gaussian Orthogonal matrix are close to the Rayleigh distribution (obeyed exactly by an ensemble of pairs of eigenvalues of 2×2 Gaussian orthogonal matrices) can be shown using less than 10 lines of

MATLAB[†] and can be computed in a few seconds. Chapter 3 introduces the theory that allows such predictions and, as its name implies, explores why such an approach should be so effective in describing the behavior of the wave-bearing and vibrating systems we are considering here.

Our third theme, *complexity* does not get a chapter to itself or even an index entry. Instead it is embedded throughout the book in the richness of the behavior of simple systems and the diversity of applications in the later chapters. Each reader will make their own connections between the various topics here, but one striking example is worth noting here: how in a multitude of contexts "the part contains the whole." Just as each cell of an organism contains the DNA of the whole being, a few short periodic orbits contain information about a large part of the eigenstructure; in seismology and underwater acoustics a short part of a time history reveals information about the whole system.

Subsequent chapters survey several applied topics related in varying degrees to the earlier chapters. Inasmuch as multiple scattering plays such a recurrent and important role in mesoscopics (the subject of Chapter 8), we also include a review of the, often too obscure to the non-initiate, diagrammatic methods for the theory of randomly scattered acoustics in Chapter 9. The surprising and highly applicable results of the theory of time-reversed waves are explored in Chapter 10 with particular reference to the themes of this book, which have led to important applications in ultrasonics.

Chapter 11 shows the relevance of ray chaos for long-range propagation in the ocean, whereas Chapter 12 demonstrates applications in seismology. Chapter 13 shows how random matrix theory can be applied to structural acoustics and vibrations, whereas Chapter 14 explains an alternative random matrix theory approach to the problem of estimating the likely variation in response that results from the inevitable small variations that arise in manufacturing.

It is impossible in a book of practical length to cover all the modern applications of these ideas that we might have, and we apologize to those who have noted holes in our coverage. Perhaps there will be a need for another book.

As editors we wish to thank the authors and the publishers for their patience during the unfortunately long time it has taken to turn their contributions into this book. We express our gratitude to all the publishers who granted permission for the chapter authors to reuse figures from their published articles without payment, and our greater gratitude to those who provided it as a matter of policy without being asked. We have tried to attribute all reused figures; if we have inadvertently failed to do so we would be grateful to be informed and will endeavor to correct the

[†] For the avoidance of doubt they are as follows:

```
n = 2000;
A = randn(n);
E = eig((A + A')/2);
s = diff(E).*real(sqrt(2*n - E(1:n-1).^2)/pi);
[N,x] = hist(s,40);
bar(x,N/n/(x(2) - x(1)))
hold on
plot(x,(pi/2)*x.*exp((-pi/4)*x.^2),'r','LineWidth',2)
hold off
```

oversight in future editions if there are any. We also wish to thank the organizers of the 2005 Summer School on Chaotic and Random Wave Scattering at the Centro International de Ciencias A. C. in Cuernavaca, at which the idea for this book was born when we accidentally got separated from the rest of our party while exploring the pyramids of Xochicalco and their notable acoustics.

Matthew Wright acknowledges the support provided by an EPSRC Advanced Research Fellowship during this project and thanks his colleagues at ISVR and in particular Chris Howls of the School of Mathematics for useful discussions and Carolyn and David for their tolerance and understanding. Richard Weaver thanks the US National Science Foundation for support from grant 28096. Olivier Legrand and Fabrice Mortessagne thank Valérie Doya for useful criticism and careful reading of the manuscript. Niels Søndergaard thanks Gregor Tanner for valuable discussions. Joseph Turner and Goutam Ghoshal gratefully acknowledge the financial support of the US Department of Energy, the National Science Foundation, and the Federal Railroad Administration. Steven Tomsovic and Michael Brown thank Javier Beron-Vera, Nicholas Cerruti, Katherine Hegewisch, Irina Rypina, and Ilya Udovydchenkov for the benefit of many discussions relating to the material presented and gratefully acknowledge support from the US National Science Foundation, grants PHY-0555301 (ST) and CMG-0417425 (MB), and Code 321 of the Office of Naval Research (MB).

1 The Semiclassical Trace Formula

Matthew Wright

Institute of Sound and Vibration Research, University of Southampton, UK

1.1 Introduction

For a two-dimensional enclosure, such as a membrane or the cross section of an infinitely long duct, those with the very simplest shapes (circles, rectangles, spheres, boxes, etc.) with simple uniform boundary conditions, the modes and natural frequencies can be determined analytically. For any other shape they may be determined numerically by a range of mature numerical techniques of which finite element and boundary element analyses are the best known and the most widely studied. Knowing how to calculate the modes and natural frequencies for any particular shape, however, is not the same as understanding how those modes and natural frequencies depend on the shape. Suppose, for example, that we wish to improve the design of a component by optimizing some quantity such as weight, while leaving its natural frequencies unchanged. In the course of such an optimization changes will be made to the shape, whereupon the process of calculating the modes and natural frequencies must begin all over again; at best, part of the mesh can be re-used. Such an analysis cannot tell us where effort can be most or least profitably concentrated.

It turns out that the shapes that can be analyzed are (for good reason) quite untypical compared with arbitrary shapes. The situation mirrors the one that used to prevail in the study of dynamical systems, where linear differential equations were most widely studied because of their solubility, and the fact that other systems showed radically different qualitative behavior was, for a time, ignored. In both cases the overlooked feature is chaos, but in the case of acoustic morphology the phenomenon is known as quantum chaos. Despite its name, this phenomenon can be exhibited by large-scale systems such as acoustical resonators, whose governing equations are entirely linear. It arises when a ray path is unstable to small perturbations and displays strong sensitivity to initial conditions.

Several surveys (Berry 1987, Guhr et al. 1998, Galdi et al. 2005, Kuhl et al. 2005) and books (Gutzwiller 1990, Ott 1993, Brack & Bhaduri 1997, Stöckmann 1999, Richter 2000, Haake 2001, Nakamura & Harayama 2004, Reichl 2004, Cvitanović et al. 2005) on aspects of this subject have become available in recent years, but these are variously intended for physicists, mathematicians, and electronic engineers. The theory of periodic orbits, and of quantum chaos, is applicable to a far greater range of areas than just acoustics, and naturally these texts span that range.

1.2 Introductory Examples

1.2.1 Modes in a Rectangular Enclosure

The rectangle is perhaps the simplest case to study because an explicit formula exists for its natural frequencies. From here on we shall work with wavenumber rather than frequency, and so we shall use the equation for the eigenwavenumbers of a rectangle with sides a_1, a_2:

$$k_{n,m} = \pi \left(\frac{n^2}{a_1^2} + \frac{m^2}{a_2^2} \right)^{1/2}, \tag{1.1}$$

where the indices n and m run $0, 1, 2, \ldots$ for Neumann boundary conditions and $1, 2, 3, \ldots$ for Dirichlet conditions. The spectral density of this system is defined as

$$\rho(k) = \sum_{n,m} \delta(k - k_{n,m}) \tag{1.2}$$

and the modecount as

$$N(k) = \int_0^k \rho(k')\,\mathrm{d}k' = \sum_{n,m} \mathrm{H}(k - k_{n,m}), \tag{1.3}$$

where H is the Heaviside function. We shall now show how alternative, series-form expressions for $\rho(k)$ and $N(k)$ can be obtained.

The delta functions in (1.2) can be written as the limit of a Gaussian function

$$\delta(k - k_{n,m}) = \lim_{t \to 0} \frac{1}{2\sqrt{\pi t}} \mathrm{e}^{-(k-k_{n,m})^2/4t}. \tag{1.4}$$

We can therefore write the spectral density function in the form

$$\rho(k) = \sum_{n=1}^{\infty} \sum_{m=1}^{\infty} \lim_{t \to 0} \frac{1}{2\sqrt{\pi t}} \mathrm{e}^{-\left(k - \pi\sqrt{n^2/a_1^2 + m^2/a_2^2}\right)^2/4t}. \tag{1.5}$$

The Poisson formula for a double sum,

$$\begin{aligned} \sum_{n=0}^{\infty} \sum_{m=0}^{\infty} f(n,m) = &\sum_{M_1=-\infty}^{\infty} \sum_{M_2=-\infty}^{\infty} \iint_0^{\infty} f(n_1, n_2) \mathrm{e}^{2\pi \mathrm{i}(M_1 n_1 + M_2 n_2)}\,\mathrm{d}n_1\,\mathrm{d}n_2 \\ &+ \frac{1}{2} \sum_{M_1=-\infty}^{\infty} \int_0^{\infty} f(n_1, 0) \mathrm{e}^{2\pi \mathrm{i} M_1 n_1} \mathrm{d}n_1 \\ &+ \frac{1}{2} \sum_{M_2=-\infty}^{\infty} \int_0^{\infty} f(0, n_2) \mathrm{e}^{2\pi i M_2 n_2} \mathrm{d}n_2 \\ &+ \frac{1}{4} f(0,0), \end{aligned} \tag{1.6}$$

can be applied to (1.5). We shall take each term separately, denoting them F_1, F_2, F_3, F_4.

The expression for F_1 can be integrated by making the substitutions

$$n_1 = \frac{a_1 r}{\pi} \cos\theta, \qquad n_2 = \frac{a_2 r}{\pi} \sin\theta, \qquad \mathrm{d}n_1\,\mathrm{d}n_2 = \frac{a_1 a_2}{\pi^2} r\,\mathrm{d}r\,\mathrm{d}\theta, \tag{1.7}$$

giving

$$F_1 = \sum_{M_1=-\infty}^{\infty} \sum_{M_2=-\infty}^{\infty} \int_0^{\infty} \int_0^{\pi/2} \lim_{t\to 0} \frac{a_1 b_1}{\pi^2} \frac{1}{2\sqrt{\pi t}} \mathrm{e}^{-(k-r)^2/4t+2\mathrm{i}(M_1 a_1 \cos\theta + M_2 a_2 \sin\theta)r} r \,\mathrm{d}r\,\mathrm{d}\theta. \tag{1.8}$$

After some manipulation this gives

$$F_1 = \frac{a_1 a_2 k}{2\pi} \sum_{M_1=-\infty}^{\infty} \sum_{M_2=-\infty}^{\infty} \mathrm{J}_0(k L_{M_1,M_2}), \tag{1.9}$$

where $L_{M_1,M_2} = 2\sqrt{M_1^2 a_2^2 + M_2^2 a_2^2}$ and J_0 is a Bessel function of zero order.

For F_2 we have

$$\begin{aligned} F_2 &= -\frac{1}{2} \sum_{M_1=-\infty}^{\infty} \lim_{t\to 0} \frac{1}{2\sqrt{\pi t}} \int_0^{\infty} \mathrm{e}^{-(k-\pi n_1/a_1)^2/4t + 2\pi \mathrm{i} M_1 n_1} \mathrm{d}n_1 \\ &= -\frac{1}{2} \sum_{M_1=-\infty}^{\infty} \lim_{t\to 0} \frac{a_1}{2\pi} \mathrm{e}^{2M_1 a_1 (\mathrm{i}k - 2M_1 a_1 t)} \left[1 + \mathrm{erf}\left(\frac{k + 4\mathrm{i} M_1 a_1 t}{2\sqrt{t}}\right)\right] \\ &= -\frac{a_1}{2\pi} \sum_{M_1=-\infty}^{\infty} \mathrm{e}^{2\mathrm{i}k M_1 a_1} \\ &= -\frac{a_1}{2\pi} \sum_{M_1=-\infty}^{\infty} \cos(2k M_1 a_1), \end{aligned} \tag{1.10}$$

and F_3 is the same with all subscripts 1 changed to 2 throughout. It can be shown that taking the sums on the left-hand side of (1.6) from 1 instead of 0, which would correspond to Neumann, rather than Dirichlet, boundary conditions, would reverse the sign of F_2 and F_3.

We therefore have

$$\rho(k) = \frac{a_1 a_2 k}{2\pi} \sum_{M_1,M_2=-\infty}^{\infty} \mathrm{J}_0(k L_{M_1,M_2}) \pm \sum_{i=1,2} \sum_{M=-\infty}^{\infty} \frac{a_i}{2\pi} \cos(2k M a_i) + \frac{\delta(k)}{4} \tag{1.11}$$

for Dirichlet (Neumann), conditions. Figure 1.1 shows a series of ray paths drawn in the rectangular domain, which reflect M_1 and M_2 times from the left and bottom walls, respectively, before returning to their origin with the initial heading so as to be able to repeat indefinitely. Such closed paths are called *periodic orbits*. Their length is given by L_{M_1,M_2}. This is no coincidence, as will be seen. The term $2kMa_i$ that forms the argument of the cosine in the second term can also be interpreted as the length of a ray path traveling between two parallel sides.

Because $\rho(k)$ is singular for all $k = k_n$, it must be smoothed before evaluation. In practice, we find it more convenient to work with $N(k)$, its integral with respect to k. Before evaluating this, however, we shall separate out the terms corresponding to zero-length orbits as

$$\overline{\rho}(k) = \frac{a_1 a_2}{2\pi} k \pm \frac{a_1 + a_2}{2\pi} + \frac{\delta(k)}{4}, \tag{1.12}$$

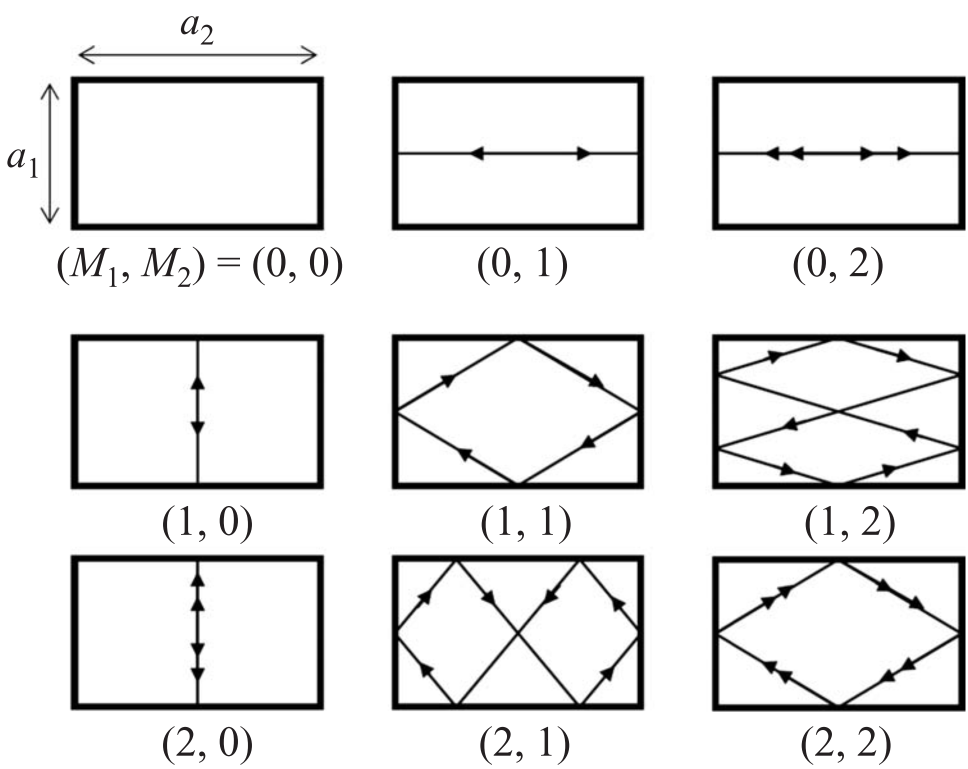

Figure 1.1. Periodic orbits for a rectangular enclosure.

leaving the remainder

$$\rho_{\mathrm{osc}}(k) = \frac{a_1 a_2 k}{2\pi} \sum_{M_1, M_2 = -\infty}^{\infty}{}' \mathrm{J}_0(k L_{M_1, M_2}) \pm \sum_{i=1,2} \sum_{M=-\infty}^{\infty}{}' \frac{a_i}{2\pi} \cos(2kMa_i), \tag{1.13}$$

where the primes on the summations indicate that the terms in which all indices are zero are omitted. The smooth components can be integrated to give

$$\begin{aligned} \overline{N}(k) &= \frac{a_1 a_2}{4\pi} k^2 \mp \frac{a_1 + a_2}{2\pi} + \frac{1}{4} \\ &= \frac{A}{4\pi} k^2 \mp \frac{L}{4\pi} k + \frac{1}{4}, \end{aligned}$$

which is the well-known formula for the average number of modes in a rectangular enclosure with area A and perimeter L (see, e.g., Morse & Ingard 1968). The oscillating component can also be integrated to give

$$N_{\mathrm{osc}}(k) = \frac{a_1 a_2 k}{2\pi} \sum_{M_1, M_2 = -\infty}^{\infty}{}' \frac{\mathrm{J}_1(k L_{M_1, M_2})}{L_{M_1, M_2}} \pm \sum_{i=1,2} \sum_{M_i = -\infty}^{\infty}{}' \frac{\sin(2k M_i a_i)}{4\pi M}, \tag{1.14}$$

where the second term can be recognized as the Fourier series representation of a sawtooth wave.

Partial sums of (1.14) plus $\overline{N}(k)$ are compared with the true modecount, calculated by evaluating (1.3) explicitly, in Figure 1.2.

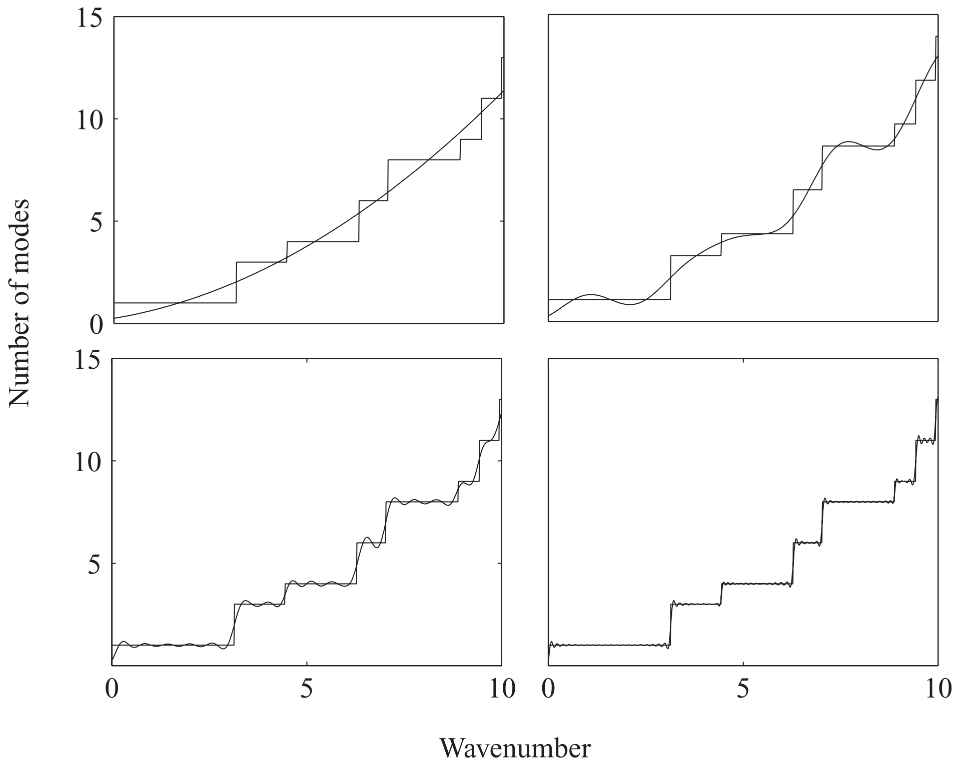

Figure 1.2. Partial sums of the semiclassical approximation to the modecount for a rectangular membrane with maximum values of M_i in all the summations of 0, 1, 4, and 20 respectively. After Wright (2001). Copyright 2001, the Acoustical Society of America.

1.2.2 The Length Spectrum of a Circle

Rather than try to derive a similar formula for the circle we will, for now, conjecture that such a formula exists and that it is of the form

$$\rho(k) \approx \sum_{\mathrm{PO}} A_{\mathrm{PO}}(k)\cos(kL_{\mathrm{PO}} + \phi_{\mathrm{PO}}), \tag{1.15}$$

where L_{PO} is the length of a periodic orbit and the sum is over all such orbits. Define the "length spectrum" $R(L)$ as the Fourier transform of $\rho(k)$. Then, if the conjecture is correct it ought to display peaks at $L = L_j$. The periodic orbits in the circle are shown in Figure 1.3, parameterized by v, the number of vertices, and w, the winding number about the center. The length of each orbit is given by

$$L_{vw} = 2vR\sin\frac{\pi w}{v}, \tag{1.16}$$

where R is the radius of the circle, taken to be unity henceforth.

Because the eigenwavenumbers of the circular membrane are zeros of Bessel functions, which can be found numerically, the length spectrum can be easily calculated as

$$R(L) = \int_{-\infty}^{\infty} \sum_{m,n} \delta(k - \mathrm{j}_{mn}) \mathrm{e}^{\mathrm{i}kL}\,\mathrm{d}k = \sum_{m,n} \mathrm{e}^{\mathrm{i}\,\mathrm{j}_{mn} L}. \tag{1.17}$$

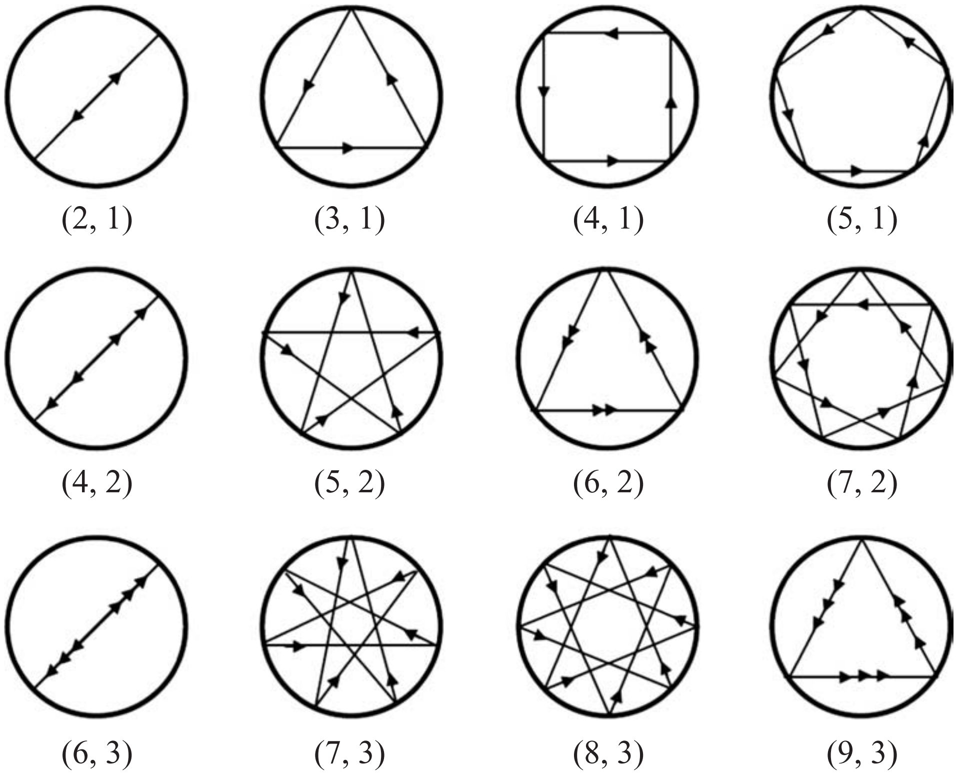

Figure 1.3. Periodic orbits for a circular domain. After Balian and Bloch (1972).

The absolute value of this is plotted in Figure 1.4. As expected from the preceding conjecture, it shows peaks at values of L satisfying Equation (1.16) for integer v and w, that is, 4, $3\sqrt{3}$, $4\sqrt{2}$, $10\sin\pi/5$, and so on.

With this evidence we are ready to sketch the derivation of a formula like Equation (1.15) for any shape of membrane or cavity. First, however, we will find it helpful to review the quantum theory that gave rise to this result, and the analogy between quantum billiards and acoustical systems.

1.3 The Quantum–Acoustic Analogy

A widely studied problem in quantum physics is that of a scalar particle in a potential field, which obeys Schrödinger's equation:

$$\frac{-\hbar^2}{2m}\nabla^2\psi_n + V(\mathbf{r})\psi_n = E_n\psi_n, \tag{1.18}$$

where $2\pi\hbar = 6.6 \times 10^{-34}$ Js is Planck's constant, m is the particle's mass, V is the potential at a point $\mathbf{r}$, and E_n is the nth discrete energy level. The complex wavefunction ψ_n can then be interpreted so that $|\psi_n(\mathbf{r})|^2\,\mathrm{d}\mathbf{r}$ is the probability of finding a particle with energy E_n in the volume $\mathrm{d}\mathbf{r}$ surrounding the point $\mathbf{r}$. If the potential takes the form of an infinite well, so that it is zero within a domain B and infinite outside it, then the boundary condition will be $\psi_n = 0$ on ∂B, and the wavefunctions will be normalized such that $\int_B |\psi_n(\mathbf{r})|^2\,\mathrm{d}\mathbf{r} = 1$ because the particle must exist

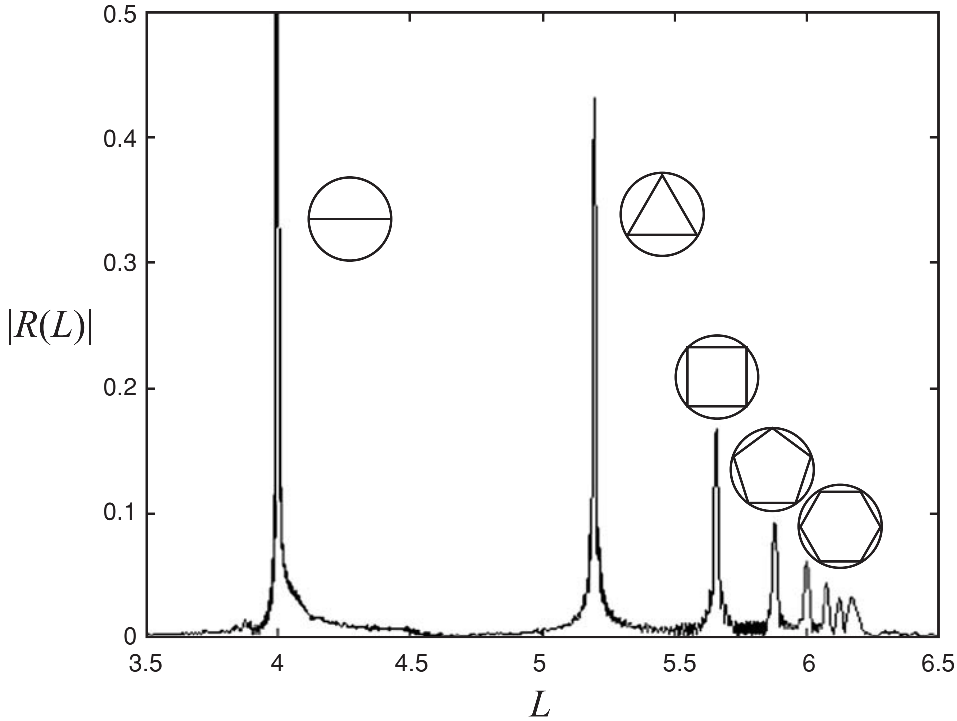

Figure 1.4. Normalized length spectrum of a circle. Periodic orbits have been sketched next to the peaks to which they correspond.

somewhere within B. Such a domain–particle system is known as a quantum billiard. The allusion is specifically to billiards (strictly carom billiards) rather than, say, snooker because in the closed systems studied here there are no pockets by which the particle can leave the domain. Open systems are considered in Chapter 6.

Because the potential is zero inside B we can rewrite Equation (1.18) as

$$\nabla^2 \psi_n + \frac{2m}{\hbar^2} E_n \psi_n = 0, \tag{1.19}$$

which is identical in form to the Helmholtz equation

$$\nabla^2 \psi_n + k_n^2 \psi_n = 0. \tag{1.20}$$

Therefore the problem of quantizing the energy levels of a two-dimensional billiard is the same as that of finding the modal frequencies of a membrane of the same shape.

1.3.1 The Semiclassical Limit

Physically, Planck's constant $\hbar$ determines the scale over which the energy levels are quantized. It is because it is very small in everyday units that quantum effects are not observed in everyday motions. Although it is a universal constant, it is convenient to allow it to vary by rescaling other quantities. As $\hbar$ becomes small, quantum effects become less noticeable, and the behavior of the system gets closer to that predicted by classical physics as $\hbar \to 0$. The behavior never becomes exactly classical, however, because this limit is singular, as can be seen by setting $\hbar = 0$ in Equation (1.19). The limiting behavior as $\hbar \to 0$ is therefore called semiclassical and corresponds to $E_n \to \infty$ in Equation (1.19) or $k_n \to \infty$ in the Helmholtz equation. In this short-wavelength limit, wave motion can be modeled by rays.

1.3.2 How to Read the Quantum Literature

The semiclassical periodic orbit theory may be of interest to acousticians because it is applicable to the Schrödinger Equation (1.18) and hence to the Helmholtz Equation (1.20). But in fact it is applicable to a much wider class of systems, namely, any system described by Hamilton's equations, that is, any conservative dynamic system. It has been usefully applied to celestial dynamics, surface science, and much more. It is only natural, therefore, that the literature is usually couched in these terms of general Hamiltonian systems, of which billiards are an example, generally considered useful for illustrating theoretical aspects, and for which numerical results can be easily computed, rather than objects of interest in their own right.

In order to interpret the quantum billiard literature in terms that are convenient for acousticians the following transformations are useful. Direct comparison of Equations (1.19) and (1.20) gives

$$E = \frac{\hbar^2 k^2}{2m} \tag{1.21}$$

in a zero potential. If $\tilde{\rho}(E)$ is the spectral density as a function of energy, then

$$\rho(k) = \frac{\hbar^2 k}{m} \tilde{\rho}(E). \tag{1.22}$$

Because of wave–particle duality the momentum p of the particle is $\hbar k$. Because the speed of the particle is the ratio of its momentum to its mass, the time period T of a path or orbit is given by

$$T = \frac{mL}{\hbar k}. \tag{1.23}$$

Finally, the action S of a path or orbit is

$$S = pL = \hbar k L. \tag{1.24}$$

Using these expressions it should be possible to evaluate the expressions appearing in the quantum billiard literature in such a way as to eliminate S, p, E, m and $\hbar$ and recover a formula that is applicable to the acoustics of membranes and cavities.

As has been pointed out by van Tiggelen (2005) the quantum–acoustic analogy, even between a membrane and a two-dimensional billiard, is not perfect. In the acoustic case the wave function ψ is the directly measurable quantity, whereas in the quantum case, only $|\psi|^2$ can be observed. In lossless acoustics, energy is conserved, whereas probability is conserved in the quantum case; that is, the eigenfunctions are normalized such that

$$\int_B |\psi|^2 \, \mathrm{d}^d \mathbf{x} = 1, \tag{1.25}$$

that is, the particle must be found somewhere in the d-dimensional billiard B.

The concept of *integrability* of a shape is important to the subject but hard to define without reference to the Hamiltonian of a point particle in a billiard of that shape, in which case it means that there are as many constants of the classical motion as there are degrees of freedom. In practice it is sufficient but not necessary for the wave equation to be separable in a particular shape of enclosure for the dynamics of a particle in it to be integrable. An example of a non-separable but integrable shape is the equilateral triangle. Other irregular polygons belong to the class known as *pseudo-integrable* (Richens & Berry 1981). Shapes that are neither integrable nor pseudo-integrable may exhibit chaotic ray dynamics, which is discussed in the next chapter.

1.4 The Semiclassical Trace Formula

The membrane has a Green's function G satisfying

$$\nabla^2 G + k^2 G = \delta(\mathbf{r} - \mathbf{r}_0) \quad \text{in } B, \tag{1.26}$$

$$G(\mathbf{r}, \mathbf{r}_0; k) = 0 \qquad \mathbf{r}, \mathbf{r}_0 \text{ on } \partial B. \tag{1.27}$$

The Green's function describes wave propagation from $\mathbf{r}$ to $\mathbf{r}_0$ and can be related to G_0, the Green's function for free space, by writing the following double-layer potential (Filippi et al. 1989):

$$G(\mathbf{r}, \mathbf{r}_0; k) = G_0(\mathbf{r}, \mathbf{r}_0; k) + \int_{\partial B} \frac{\partial G_0(\mathbf{r}, \alpha)}{\partial n_\alpha} f(\alpha, \mathbf{r}_0)\, \mathrm{d}\sigma_\alpha, \tag{1.28}$$

where f is to be determined. Balian and Bloch (1972)observed that the solution can be found by successive approximation as follows:

$$\begin{aligned} G(\mathbf{r}, \mathbf{r}_0; k) = {} & G_0(\mathbf{r}, \mathbf{r}_0; k) \\ & - 2 \int\limits_{\partial B} \frac{\partial G_0(\mathbf{r}, \alpha)}{\partial n_\alpha} G_0(\alpha, \mathbf{r}_0)\, \mathrm{d}\alpha \\ & + 2^2 \iint\limits_{\partial B \times \partial B} \frac{\partial G_0(\mathbf{r}, \alpha)}{\partial n_\alpha} \frac{\partial G_0(\alpha, \beta)}{\partial n_\beta} G_0(\beta, \mathbf{r}_0)\, \mathrm{d}\alpha\, \mathrm{d}\beta \\ & - 2^3 \iiint\limits_{\partial B \times \partial B \times \partial B} \frac{\partial G_0(\mathbf{r}, \alpha)}{\partial n_\alpha} \frac{\partial G_0(\alpha, \beta)}{\partial n_\beta} \frac{\partial G_0(\beta, \gamma)}{\partial n_\gamma} G_0(\gamma, \mathbf{r}_0)\, \mathrm{d}\alpha\, \mathrm{d}\beta\, \mathrm{d}\gamma \\ & + \cdots, \end{aligned} \tag{1.29}$$

where each successive integral corresponds to another reflection of waves from the boundary; because the waves spread in all directions the integrations are around the entire boundary. In the semiclassical limit the Green's function will tend to its large argument asymptote; for example, in two dimensions

$$G_0(\mathbf{r}, \mathbf{r}_0; k) = \frac{1}{4\mathrm{i}} \mathrm{H}_0^{(1)}(k|\mathbf{r} - \mathbf{r}_0|) \sim -\frac{(1+\mathrm{i})}{4\sqrt{\pi k |\mathbf{r} - \mathbf{r}_0|}}\, \mathrm{e}^{\mathrm{i}k|\mathbf{r}-\mathbf{r}_0|}, \quad \text{as } k \to \infty, \tag{1.30}$$

where $\mathrm{H}_0^{(1)}$ is the zero-order Hankel function of the first kind. Whatever the number of dimensions the Green's function will behave like a complex exponential at large argument, and therefore the integrals in Equation (1.29) will all take the form

$$\int \cdots \int g(\mathbf{r}) \mathrm{e}^{\mathrm{i}k|\mathbf{r}-\mathbf{r}_0|}\, \mathrm{d}\alpha \cdots \mathrm{d}\omega,$$

in which case the method of stationary phase (Self 2005) can be used. Under this approximation, each integral will be dominated by the contribution from specularly reflecting paths and the semiclassical approximation to the Green's function will be

$$G(\mathbf{r}, \mathbf{r}_0) \approx \sum_j a_j(\mathbf{r}, \mathbf{r}_0) \mathrm{e}^{\mathrm{i}kL_j + \mathrm{i}\phi_j}, \tag{1.31}$$

where a_j is a geometrical prefactor, which can be obtained from the geometry of the orbit; L_j is the length of specularly reflecting ray paths; and ϕ_j, known as the Maslov phase, is related to phase changes undergone by a ray in traversing the path of length L_j.

Consider now the exact spectral density of the system, defined by

$$\rho(k) = \sum_{n=0}^{\infty} \delta(k - k_n). \tag{1.32}$$

This can be related to the Green's function of the system by the trace formula

$$\rho(k) = -\frac{1}{\pi} \lim_{\epsilon \to 0} \Im \left\{ \int_B G(\mathbf{r}, \mathbf{r}; k + \mathrm{i}\epsilon)\, \mathrm{d}\mathbf{r} \right\}, \tag{1.33}$$

where $G(\mathbf{r}, \mathbf{r}; k)$ is known as the trace Green's function, which is singular for $k = k_n$, necessitating the limiting process. The spectral density can be written as the sum of a smooth part and an oscillatory part:

$$\rho(k) = \overline{\rho}(k) + \rho_{\mathrm{osc}}(k), \tag{1.34}$$

and substituting the semiclassical Green's function of Equation (1.31) into Equation (1.33) gives the semiclassical trace formula

$$\rho(k) \approx \overline{\rho}(k) + \sum_j A_j(k) \mathrm{e}^{\mathrm{i}kL_j + \mathrm{i}\phi_j} + \cdots, \tag{1.35}$$

where L_j is the length of the jth periodic orbit, A_j gives the amplitude of its contribution (discussed later), and ϕ_j is the phase change accumulated over one period. The value of this expression is that it quantifies the effect of the geometry on the spectrum through A_j and L_j and those of the type of boundary conditions through ϕ_j. This is, in principle, true for a very wide class of shapes* and in particular does not depend on separability, though convergence of the series is not guaranteed in all cases for which such a formula can be obtained. Furthermore the fact that the geometry and boundary conditions enter the formula through different variables means that once the periodic orbits have been determined for a particular shape the approximate spectrum can be determined for any boundary condition type.

* When the shape is near to an integrable shape the relevant formula takes a different form (Tomsovic et al. 1995, Ullmo et al. 1996). For systems with mixed chaoticity the question is still open.

1.4.1 Smooth Spectral Density and Modecount

The smooth part of the spectral density, and hence the smooth modecount, has been extensively reviewed by Baltes and Hilf (1976). The relevant results can be briefly summarized: first for two dimensions,

$$\overline{N}(k) = \frac{|B|}{4\pi}k^2 \pm \frac{|\partial B|}{4\pi}k + \left[\frac{1}{12\pi}\int_B K(s)\,\mathrm{d}s + \frac{1}{24\pi}\sum_i\left(\frac{\pi}{\alpha_i} - \frac{\alpha_i}{\pi}\right)\right] + O(k^{-1}), \tag{1.36}$$

where $|B|$ and $|\partial B|$ are the area and boundary length of the domain, $K(s)$ is the radius of curvature as a function of distance s along the boundary, and α_i is the included angle of the ith corner. In three dimensions the corresponding expression is

$$\overline{N}(k) = \frac{|B|}{6\pi^2}k^3 \pm \frac{|\partial B|}{16\pi}k^2 + \left[\frac{1}{24\pi}\sum_i\left(\frac{\pi}{\alpha_i} - \frac{\alpha_i}{\pi}\right)L_i\right]k + O(k^0), \tag{1.37}$$

where $|B|$ and $|\partial B|$ are now the volume and surface area and L_i is the length of the ith edge with included angle α_i. The leading term of these expressions is called the Weyl law; the full series is often called the Weyl series.

One way to examine how closely the eigenvalues of a particular system adhere to the predictions of the Weyl series would be to calculate both N and $\overline{N}$ and plot one against the other. A similar effect, however, can be obtained with a discrete set by examining the values of $x_n = \overline{N}(k_n)$. This procedure is known as "unfolding the spectrum." The expected value of x_n is $n - (1/2)$, and a graph of the staircase obtained from x_n (in the same way that N is obtained from k_n) has the same form as a graph of N versus $\overline{N}$. In this way it is straightforward to compare the departures from the average of eigenvalues from different systems with one another and to examine phenomena such as spectral rigidity, as will be explored in the following chapter.

1.5 The Nature of the Approximation

It is only in very rare circumstances, such as for the rectangle, that an exact expression in terms of periodic orbits can be found. More usually when rules to find the amplitude and phase terms (discussed in Section 1.6) are followed, the result is an approximation. There are two reasons for this approximation: first that only the leading-order semiclassical approximation to the Green's function is used (though this will only be the case in two dimensions) and second that the method of steepest descent has been applied. This second source of approximation is the dominant one and means that only terms to leading order in k are obtained. Furthermore, the formula is only asymptotically true as $k \to \infty$.

It might be thought that this means that the trace formula is only useful at very high frequencies. However, the number of periodic orbits needed to resolve steps in the modecount function increases rapidly with wavenumber. This means, as noted by Fulling (2002), that the trace formula is more useful at low frequencies. This "proliferation of orbits" is even more marked in the chaotic shapes to be considered later than it is for the integrable shapes considered so far and in the next section. Furthermore, convergence of the series is only likely in the case of integrable or pseudo-integrable shapes.

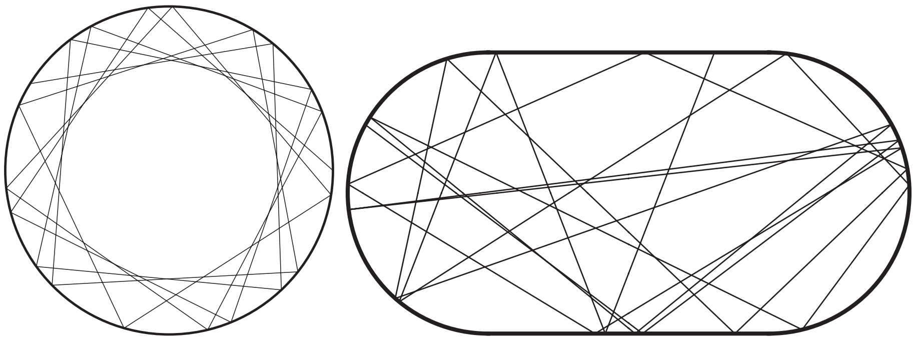

Figure 1.5. Two widely studied billiards. The ray dynamics in the circle are integrable, and all its periodic orbits are marginally stable and lie in continuous families. It was proven by Bunimovich (1974) that the ray dynamics in the stadium are entirely chaotic. All its periodic orbits are unstable, and all are isolated with the exception of the “bouncing ball” orbits that run perpendicularly between the two straight sides.

Boasman (1994) examined the accuracy of the semiclassical approximation within the context of the boundary integral method and found it to be good. Primack and Smilansky (1998) showed that the accuracy of the semiclassical trace formula depends only weakly, if at all, on dimensionality.

1.6 Derivation of Trace Formulas for Given Shapes

A number of methods have been developed to calculate expressions for the amplitude and phase terms in the trace formula. They are as follows:

(i) Gutzwiller’s (1970) method for isolated orbits, which involves determining the stability matrix for each orbit;
(ii) Balian and Bloch’s (1972) method, based on multiple reflections, which derives amplitude terms for a wide range of conditions in a three-dimensional billiard;
(iii) Berry and Tabor’s (1976) method for integrable Hamiltonian systems, based on action-angle variables (these are developed in Chapter 11); and
(iv) Creagh and Littlejohn’s (1991, 1992) generalization of Gutzwiller’s method to include continuous families of orbits.

We will concentrate on the last of these because of its wide applicability and because it highlights the geometry of the orbits. Balian and Bloch (1972) gave a worked example of the application of the first method to a sphere, whereas worked examples for a circle were given using the second method by Richter et al. (1996), and using the third method by Creagh (1996).

1.6.1 Billiard Dynamics

The dynamics of billiards is a large subject that was first studied by Birkhoff (1927) and has since been treated in a number of surveys and monographs (Kozlov & Treshchëv 1980, Gutkin 2003, Tabachnikov 2005). Here only the elements necessary to the trace formula will be developed. Two widely studied billiards are shown in Figure 1.5; it is clear that the dynamics in the circle and the stadium are very different.

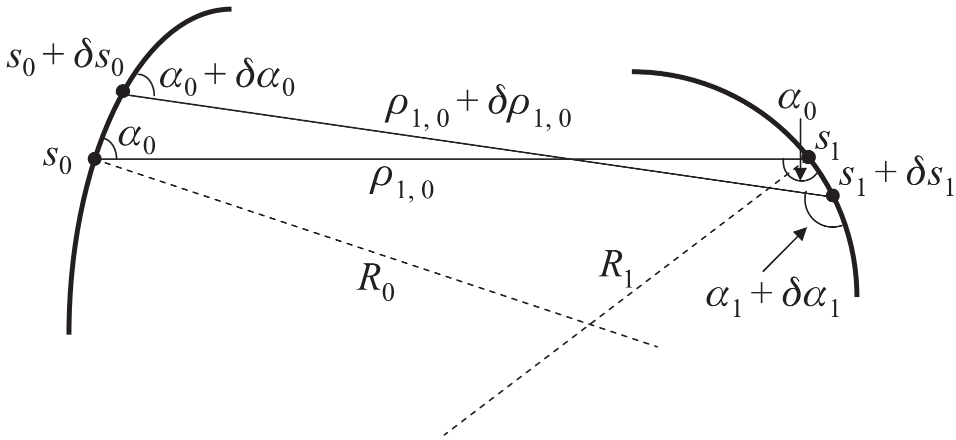

Figure 1.6. A segment of a periodic orbit between two bounces labeled 0 and 1.

The dynamics of any billiard can be characterized by taking its boundary as a Poincaré surface of section because between bounces the motion of the particle is completely determined. For some plane billiard B, let s denote the distance around its boundary from some chosen origin. Let s_n be the location of the nth bounce and α_n the angle between the path of the particle/ray and the tangent to the billiard wall at the point of impact. These two discrete variables completely define the particle/ray path, but we prefer to use $p_n = \cos\alpha_n$ for two reasons: first because it corresponds to a component of the momentum of a particle that is of physical interest in quantum mechanical problems, and it is convenient for us to follow the same notation; second because the nonlinear mapping M of the phase space $(s, p)^T$ induced by the billiard and defined by

$$\begin{pmatrix} s_{n+1} \\ p_{n+1} \end{pmatrix} = M \begin{pmatrix} s_n \\ p_n \end{pmatrix} \tag{1.38}$$

is area preserving. These coordinates define the phase space for the dynamics in the billiard. To study the dynamics we need to study the stability of rays to small perturbations, which is governed by the stability matrix.

1.6.2 Stability Matrix

The following procedure for evaluating the stability matrix directly from the orbits has been given by Berry (1981b) and in appendix C of Brack and Bhaduri (1997). Consider a part of an orbit that makes two successive bounces with the boundary, which we can number 0 and 1 without loss of generality (see Figure 1.6). The stability matrix depends on the stability of the orbit, which can be investigated by making a small change to point 0 and examining the resulting change in point 1. In the limit of small changes the transformation will be linear and can be written as

$$\begin{pmatrix} \delta s_1 \\ \delta\cos\alpha_1 \end{pmatrix} = \mathbf{M}_{1,0} \begin{pmatrix} \delta s_0 \\ \delta\cos\alpha_0 \end{pmatrix}. \tag{1.39}$$